ORIGINAL RESEARCH

Neuromuscular Polytrauma Pain is Resolved by Macrophage COX-2 Nanoimmunomodulation

Ibdanelo Cortez[1],*, Caitlyn M Gaffney[1],*, Riddhi Vichare[2], Caitlin V Crelli[2], Lu Liu ⓘ[2], Eric Lee ⓘ[1], Jules Edralin[1], James M Nichols[1], Hoang Vu Pham[1], Syed Mehdi[1], Jelena M Janjic ⓘ[2], Andrew J Shepherd ⓘ[1]

[1]Laboratories of Neuroimmunology, Department of Symptom Research, the University of Texas MD Anderson Cancer Center, Houston, TX, 77030, USA; [2]School of Pharmacy, Duquesne University, Pittsburgh, PA, 15282, USA

*These authors contributed equally to this work

Correspondence: Jelena M Janjic, School of Pharmacy, Duquesne University, 600 Forbes Ave., Pittsburgh, PA, 15282, USA, Email janjicj@duq.edu; Andrew J Shepherd, Laboratories of Neuroimmunology, Department of Symptom Research, the University of Texas MD Anderson Cancer Center, Unit 1055, 6565 MD Anderson Boulevard, Houston, TX, 77030, USA, Tel +1 713 745-7959, Fax +1 832 750-5153, Email ajshepherd@mdanderson.org

Abstract: Soft tissue injuries often involve muscle and peripheral nerves and are qualitatively distinct from single-tissue injuries. Prior research suggests that damaged innervation compromises wound healing. To test this in a traumatic injury context, we developed a novel mouse model of nerve and lower limb polytrauma, which features greater pain hypersensitivity and more sustained macrophage infiltration than either injury in isolation. We also show that macrophages are crucial mediators of pain hypersensitivity in this model by delivering macrophage-targeted nanoemulsions laden with the cyclooxygenase-2 (COX-2) inhibitor celecoxib. This treatment was more effective in males than females, and more effective when delivered 3 days post-injury than 7 days post-injury. The COX-2 inhibiting nanoemulsion drove widespread anti-inflammatory changes in cytokine expression in polytrauma-affected peripheral nerves. Our data shed new light on the modulation of inflammation by injured nerve input and demonstrate macrophage-targeted nanoimmunomodulation can produce rapid and sustained pain relief following complex injuries.

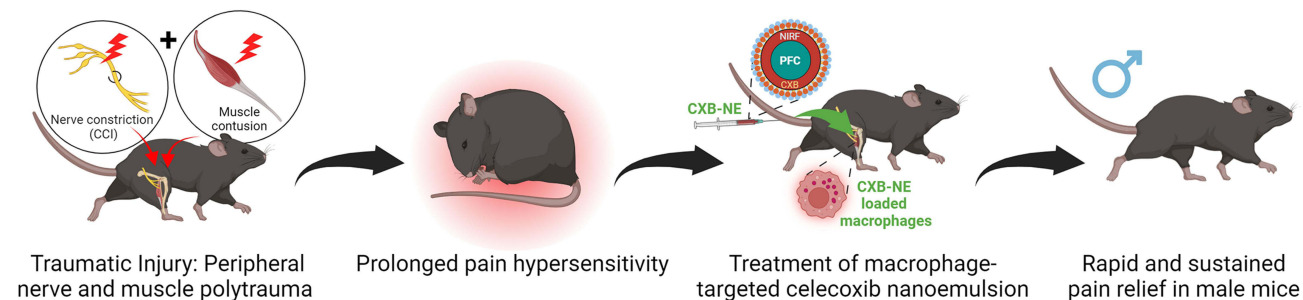**Keywords:** nerve injury, muscle contusion, inflammation, celecoxib, nanoemulsion, COX-2

Introduction

Deficient tissue healing following traumatic injury is linked to chronic pain.[1] Although soft tissue repair following injury is predominantly macrophage-driven, a failure of macrophages to transition from a pro-inflammatory to anti-inflammatory phenotype has been implicated in non-resolving inflammation and sustained pain.[2–6] Skeletal muscle repair after contusion requires a series of highly coordinated events that are modulated by macrophages. Activated by damaged myofibers, intramuscular macrophages are responsible for removing dead cells immediately following injury and initiating muscle regeneration by signaling to satellite cells, fibroblasts, and other immune cells.[7–10] Additionally, crosstalk with the peripheral nervous system orchestrates immune responses to injury, and in particular macrophages. This relationship has been observed in the skin[11–13] and the peripheral nervous system.[14–17]

We recently showed that lower limb muscle contusion is associated sustained pain hypersensitivity, but only relatively transient macrophage infiltration of muscle and overlying skin/fascia. Instead, we observed sustained macrophage infiltration of the ipsilateral sciatic nerve which was closely associated with the sustained pain hypersensitivity observed.[18] This suggested that in soft tissue injuries, concomitant macrophage infiltration of said nerve may be an important driver of sustained pain. Prior studies suggest that disruption of somatosensory input to tissue impairs innate immune-dependent healing in different chronic pain models, thereby sustaining pain hypersensitivity.[13]

Since traumatic injury often involves both soft tissue injury and damage to the somatosensory nervous system, we hypothesized that polytrauma to the lower limb and its associated nerve input would produce inflammation and pain

Graphical Abstract

Traumatic Injury: Peripheral nerve and muscle polytrauma

Prolonged pain hypersensitivity

Treatment of macrophage-targeted celecoxib nanoemulsion

Rapid and sustained pain relief in male mice

hypersensitivity that would be distinct from either injury in isolation.[19–21] To test this hypothesis, we developed a model in which a mild nerve constriction (single-ligature chronic constriction injury; CCI) was paired with a mild lower limb contusion. Sciatic nerve constriction is an established model for neuropathic pain that is improved with anti-inflammatory drugs.[22–24] The single-ligature variation induces relatively mild mechanical hypersensitivity compared to the more standard four ligatures.[25] Since the polytrauma model shows extensive macrophage accumulation at both sites of injury, we also investigated whether they could be targeted for macrophage-specific nanoimmunomodulation[26] and resultant pain relief. In the previous work, we showed that macrophage-specific nanoimmunomodulation markedly reduces mechanical hypersensitivity in rodent nerve injury pain models by reducing both macrophage infiltration and release of pro-inflammatory mediators at the injury site.[27,28] Non-steroidal anti-inflammatory drug (NSAID)-loaded nanoemulsions attenuated neuropathic pain in a CCI rat model[27,28] and inflammatory pain in a CFA mouse model.[29] Nevertheless, the contribution of macrophages to muscle injury and polytrauma was not investigated.

We have reported in earlier studies that nanoemulsion-based nanotherapeutics, formulated as colloidal dispersions of oil in buffered aqueous media, can incorporate both lipophilic fluorescent dyes (which facilitate macrophage tracking by near-infrared fluorescence (NIRF) imaging in vivo and ex vivo)[27–30] as well as drugs.[27–29] Currently, NSAIDs such as cyclooxygenase-2 (COX-2) inhibitors are commonly used to treat musculoskeletal injuries to reduce both inflammation and pain. However, current clinical practice applies NSAIDs systemically where they substantially lack in both cellular and molecular specificity. We showed that the COX-2 inhibitor celecoxib can be packaged into a nanotherapeutic formulation, which can be used to dampen inflammation and pain by specifically reducing prostaglandin synthesis in infiltrating macrophages.[27,28,30,31] The selectivity of the nanoemulsion enables retention of anti-inflammatory and analgesic efficacy[27–29,32] at markedly lower doses compared to systemic administration of the drug, reducing the potential for cardiovascular events and gastrointestinal bleeding, which are concerns with conventional celecoxib use.[33]

Currently, there are no studies that describe the inflammatory response and pain hypersensitivity for neuromuscular polytrauma injuries in rodents. Here, we present a novel polytrauma model in mice that accounts for both muscular and neuronal injury. We characterize pain-related behaviors in this model using automated gait analysis, mechanical hypersensitivity measurements, and evaluations of grip strength while tracking macrophages that drive inflammation using NIRF imaging. To demonstrate the direct involvement of COX-2 in macrophages in the pathophysiology of pain in this model, we used COX-2 inhibitor-loaded nanoemulsions to selectively inhibit prostaglandin production from macrophages that infiltrate the sites of injury. Our data shed new light on the interactions between the somatosensory nervous system and immune system in tissue injury, revealing a crucial role for macrophages and their pro-inflammatory activity in polytrauma-driven pain.

Materials and Methods
Mice
All experiments and procedures involving the use of Mice were approved by MD Anderson Cancer Center Animal Care and Use Committee (Houston, TX, USA) in accordance with the National Research Council *Guide for the Care and Use of*

Laboratory Animals. A total of 176 male and female C57BL/6J (catalog #000664) and C57BL/6-Tg (Csf1r-EGFP-NGFR /FKBP1A/TNFRSF6)2Bck/J (Macrophage Fas-Induced Apoptosis/"MaFIA" catalog #005070) were obtained at 8 weeks from Jackson Laboratories. A total of 8 mice per group were used for von Frey and Catwalk gait analyses. In a separate cohort, 5 mice per group were used to measure grip strength and observe NIRF-NE for IVIS experiments. A total of 5 mice per timepoint for each group were used for all immunofluorescence studies, which were terminated at 3, 14 and 28 days post-injury. In celecoxib–nanoemulsion studies, mice were used as follows: 6 animals per sex and treatment were used to test a single treatment at 7 days post injury. In a separate experiment, a small group of 5 males per group were used to test a single treatment at 3 days post injury. Lastly, 5 mice per sex and treatment were used to test multiple CXB-NE treatments at 1 and 3 days post injury. IVIS images were taken of the same group of animals in the multiple treatment studies ie (N = 5 mice/sex/treatment). Mice were randomly assigned to experimental groups with an even split between males and females. Mice were maintained at the Research Animal Support Facility of MD Anderson Cancer Center (Veterinary Medicine and Surgery Department) in a 12 h light–dark cycle, with access to food and water *ad libitum*.

Muscle Contusion, CCI and Polytrauma Model

To deliver a reproducible muscle injury to mice, a Neuropactor™ traumatic brain injury instrument (Neuroscience Tools, O'Fallon, MO) was attached to a Kopf model 940 stereotaxic frame. This approach, similar to that described by Dobek et al[34] was recently described.[18] The severity of injury was adjusted by moving the electromagnetic piston head downwards onto the left hindlimb by a distance of 1 or 3 mm. All settings on the Neuropactor were kept constant: 5 m/sec velocity, with the two impacts spaced 3 mm apart overlying the gastrocnemius muscle, with 30 seconds dwell time for each impact. Animals were returned to their home cage for recovery, monitored after injury and checked daily for any complications. Mice in polytrauma and CCI groups also underwent surgery to produce constriction injury of the sciatic nerve. These mice were anesthetized using isoflurane and the left hind leg prepared as previously discussed. Mice in polytrauma studies first underwent muscle contusion, which was immediately followed by CCI surgery. To produce CCI nerve injury, a 10 mm incision was made in the skin overlying the left biceps femoris. The biceps femoris was carefully separated to expose the sciatic nerve beneath. The sciatic nerve was lifted away from surrounding muscles using sterile plastic pipette tips (200 µL) and a single 7–0 chromic gut suture (Ethicon 1745G) was loosely tied around all three branches of the sciatic nerve, proximal to the trifurcation of the nerve. A single nylon suture was used to close the overlying muscle and wound clips were applied to seal skin incision. Mice in sham surgery groups underwent incision and nerve exposure without suture application. Animals were returned to their home cage for recovery, monitored after injury and checked daily for any complications. No mice experienced adverse events as a result of the polytrauma injuries, and no mice were excluded from the study.

Von Frey Test of Mechanical Hypersensitivity

The von Frey test was carried out during the light cycle, between 08:00 and 10:00 h. Mice were tested in the same room as which they were housed. Mice were placed in single-occupancy plexiglass boxes, set on a wire mesh platform. Von Frey filaments of increasing strength (0.04–2 g) were presented to each hind paw, starting with the 0.6 g filament. Filaments were presented to the plantar surface of each hind paw and then presented with a stronger or weaker filament according to the up-down method.[35] Fifty percent paw withdrawal threshold (PWT) values were calculated for each hindpaw. Measurements were performed before injury and 3, 7, 10, 14, 21, 28, 35, 42, 49, and 56-days post-injury.

Digital Gait Analysis

Analysis of gait patterns was performed using the Catwalk® XT 10.5 system (Noldus Information Technology, Leesburg VA) as previously described.[36] Gait was measured before injury and then 3, 7, 10, 14, 21, 28 and 35-days post-injury. All habituation and testing was performed in the light cycle between 12:00 and 16:00 h. Four compliant runs were captured per mouse (run duration between 0.5 and 5 s, maximum variation in run speed <60%). Detailed descriptions for the gait indices extracted are described elsewhere[18,36] and in Additional File 1.

Macrophage Tracking by NIRF Imaging

To track macrophage accumulation non-invasively, mice received 0.2 mL of NIRF labeled DF-NE via tail vein injection 24 hours prior to injury. Mice were imaged 3, 14 and 28 days post-injury. NIRF images were captured using the IVIS Lumina system (Caliper Life Sciences; Waltham, MA) using the auto exposure setting (≤40 sec). Fluorescence from the DiR component of the emulsion was detected with a 745 nm (bandpass: 20 nm) excitation and 800 nm (bandpass: 35 nm) emission filter. After obtaining images from each mouse, regions of interest were drawn around each hindlimb and the Average Radiant Efficiency ([p/s/cm²/sr] / [μW/cm²]) was obtained for each. To account for minor animal-to-animal variability in fluorescence, values are expressed as the ratio of radiant efficiency in the ipsilateral versus contralateral hindlimb.

Tissue Collection and Sectioning

Mice were euthanized using CO_2 and perfused with 10 mL of cold 0.1 M PBS followed by 10 mL of cold 4% PFA (Thermo Scientific; Waltham, MA). Sciatic nerves were collected by cutting distally at the knee and proximally to the spinal cord. Gastrocnemius muscle and overlying skin/fascia, sciatic nerves and dorsal root ganglia were post-fixed overnight at 4°C in 4% PFA. Tissues were then transferred to 30% sucrose for two days at 4 °C, and subsequently embedded in Tissue-Tek® OCT compound (Sakura; Torrance, CA) for cryosectioning. Transverse sections of gastrocnemius muscle and DRG were sectioned at 30 and 20 μm, respectively, and longitudinal sections of sciatic nerve were sectioned at 30 μm using a Leica CM3050S cryostat and collected onto Superfrost Plus slides (Fisher Scientific; Pittsburgh, PA). The sections were allowed to adhere to the slides at room temperature (RT) for approximately 10 minutes prior to storage at −20 °C, since prolonged exposure to RT adversely affected NIRF-NE fluorescence intensity.

Immunofluorescence

Slides containing sections underwent immunohistochemistry as described previously.[18,30,37] Briefly, a hydrophobic barrier was drawn on each slide using an ImmEdge™ Pen (Vector Laboratories; Burlingame, CA). After washing in 0.1 M PBS, blocking buffer (10% goat serum (Sigma), 2% bovine serum albumin (Fisher Scientific), 2% DMSO (Sigma), 1 mg/mL digitonin (Millipore; Burlington, MA) in 0.1 M PBS) was added for one hour at RT. Blocking buffer was replaced with primary antibodies diluted in blocking solution: rabbit anti-PGP9.5 (1:250; Abcam; Cat. No. ab108986 (EPR4118)), and rat anti-CD68 (1:250; Bio-Rad; Cat. No. NC9471873 (FA-11)) were added to the slides in blocking solution. The primary antibodies were incubated overnight at 4°C in a humidified slide staining chamber. The next day the slides were rinsed in 0.1 M PBS, and goat anti-rabbit Alexa Fluor 647 (1:500; Invitrogen; Carlsbad, CA), goat anti-rat Alexa Fluor 488 (1:500; Invitrogen), and DAPI (500 ng/mL; Sigma) were added to each slide in 0.1 M PBS and incubated for 3 hours at RT. Slides were washed in 0.1 M PBS, and 10% neutral buffered formalin (Thermo Scientific; Waltham, MA) was added to the sides for 10 minutes to help maintain DiI signal within NIRF-NE. The sections were washed once more in 0.1 M PBS and mounted with Prolong Gold Mounting Medium (Cell Signaling Technology, Danvers, MA).

AP20187 Treatment of MaFIA Mice

To induce macrophage depletion, MaFIA mice were treated with 3 consecutive daily injections of AP20187 (2mg/kg, i. p.) or vehicle (PBS, 10% v/v PEG-400, 1.7% v/v Tween-80). This treatment is sufficient to temporarily deplete macrophage density in skin and sciatic nerve by ≥85%.[16,38–40]

Celecoxib-Loaded Nanoemulsion (CXB-NE) Formulation

Nanoemulsions were manufactured following previously reported procedure.[41] Briefly, the M110S microfluidizer (Microfluidics Corporation, Westwood, MA) chamber was iced prior to manufacturing. CXB (50 mg) was dissolved in Miglyol 812 N and co-solubilizers transcutol and DMSO (1:1) by continuously stirring overnight. On the next day, NIRF dyes were incorporated in pre-dissolved mix (for CXB-NE). The final concentration of the micelle solution in PBS was 5% w/v, where 4.15% w/v was P105 and 0.85% w/v was P123. The pre-emulsion was then poured into the M110S inlet reservoir. The pre-emulsion was processed for 30 pulses (6 passes) at an inlet air pressure of ~80 psi and an operating liquid pressure ~17,500 psi before the final product was released from the outshoot.

Fluorescence Microscopy in Macrophages in Culture

RAW 264.7 cells were seeded at 20,000 cells per well in 0.75 mL of cell culture media on an 8-well chamber slide system Lab-TekII. After 24 h of incubation at 37 °C and 5% CO_2, the cells were treated with 20 μL/mL dose of NE for 24 h. The treatments were removed, and the chamber slides were washed with warm 1× PBS and fixed with 4% paraformaldehyde at ambient temperature for at least 20 min and washed with 0.5 mL 1× PBS twice. After removing chamber wall, 2–3 drops of mounting media with DAPI were applied. Slides were analyzed on Keyence Microscope under 700 nm and 800 nm channels.

Flow Cytometry

RAW 264.7 macrophages were plated in 12-well plates (0.2 million cells per well). After 24 h, macrophages were treated with NEs (20 μL/mL) for 3 h. Cells were washed with 1XPBS, trypsinize, and fixed at room temperature with 2% PFA in DPBS for 20 min. All experiments were performed in triplicate, and samples were analyzed using Attune Nxt (Thermo Fisher Scientific) recording 50,000 events. The nanoemulsion was detected in the RL3 (DiR, 748 nm/780 nm) channel.

Celecoxib-Loaded Nanoemulsion (CXB-NE) Injection and Imaging

A 0.2 mL of CXB-NE was injected into polytrauma mice i.v., either 7 days post-injury, 3 days post-injury, or 24 h and 3 days post-injury (ie two doses). CXB-NE injection in uninjured mice and DF-NE injection in injured mice served as negative controls. NIRF images were captured using the IVIS Lumina system as described previously.[18,30]

Confocal Microscopy and Image Quantification

Tile scans of tissue sections were obtained using a 20x objective (Numerical aperture: 0.75) on a Nikon A1R confocal microscope (Nikon Instruments Inc., Melville, NY), and image analysis was performed using Nikon NIS-Elements Advanced Research (Nikon Instruments Inc). Images are a projection of 4–5 focal planes in a 20–30 μm z-stack at 5 μm increments. Sections from at least 3 mice/experimental group were imaged. About 3–4 different sections were imaged from the same mouse. NIRF-NE / CD68 quantification was determined by drawing regions of interest around the relevant tissues and setting an intensity threshold for positive staining that was applied consistently across all images, as described previously.[30,42]

Cytokine Array Analysis

Sciatic nerves were isolated 24 hours after dosing with DF-NE or CXB-NE, and 48 hours after injury. Tissues were homogenized in RIPA buffer containing 1% Triton X-100 and Halt Protease Inhibitor Cocktail (Thermo Fisher). Lysates were then incubated with Mouse Cytokine XL Proteome Profile arrays (Biotechne) according to the manufacturer's instructions and as described previously.[30,42] Chemiluminescent signal was detected using an Amersham ImageQuant 800 blot scanner and ImageQuant TL toolbox v8.2.0 software (GE Healthcare Bio-Sciences). The mean chemiluminescent intensity for each factor was used to calculate the fold-change in abundance due to injury for each factor. Polytrauma sciatic nerves were compared against contralateral in DF-NE controls. Polytrauma sciatic was compared against contralateral nerve in CXB-NE-injected mice. Those factors with differential expression in the ipsilateral DF-NE nerve ($\pm \geq$ 2-fold) were selected for comparison.

Statistical Analysis

All behavioral and histological data are represented as mean ± standard error (SEM), and all analyses were performed using GraphPad Prism 9. All data sets were normally distributed as determined by D'Agostino & Pearson or Shapiro–Wilk tests. Differences between groups were analyzed by either two-tailed unpaired t-tests, one- or two-way repeated measures analysis of variance (ANOVA) or a mixed-effects model with Šidák's multiple comparisons test, as described in the legends of each figure $p < 0.05$ was considered statistically significant.

Results

Nerve Injury Increases Mechanical Hypersensitivity When Paired with Lower Limb Contusion

To determine the effect of nerve injury on muscle contusion pain, we first employed a 'low-severity CCI', in which the sciatic nerve was constricted using a single, absorbable 7–0 Vicryl suture (Figure 1A). CCI alone produces gradual-onset hypersensitivity in von Frey testing in the ipsilateral hindpaw, peaking at 10 days post-injury and resolving by 35 days post-injury, without any effect in the contralateral hindpaw (Figure 1B and C). The reversal of hypersensitivity at 35 days post-injury is consistent with the time reported for this suture to lose the majority of its tensile strength.[43]

To generate the polytrauma injury, we paired this version of CCI with our previously demonstrated lower limb contusion model.[18] Contusion severity was adjusted by controlling the vertical displacement of the impact piston. We generated two polytrauma groups: 1 mm contusion plus CCI ("1 mm polytrauma"; Figure 1D–F) and 3 mm contusion plus CCI ("3 mm polytrauma"; Additional Figure 1A-C) and compared against matched "contusion-only" groups (which underwent sciatic nerve exposure but not constriction). A significant interaction ((F 40, 397) = 5.29; p < 0.0001) between injury and time was observed among polytrauma groups and their respective contusion-only groups. Overall, polytrauma was associated with increased mechanical hypersensitivity compared to contusion-only and naïve control groups, though the only significant differences between injuries were on days 10–21 between 1 mm contusion-only and 1 mm polytrauma, and on day 3 and 42 between 3 mm contusion-only and 3 mm polytrauma (Figure 1E and Additional Figure 1B). Furthermore, 1 mm polytrauma and 3 mm polytrauma exhibited hypersensitivity up to 35- and 49-days post injury, respectively. Injuries did not produce any mechanical hypersensitivity in the contralateral hindpaws at any timepoint tested (Figure 1F and Additional Figure 1C).

Transient Gait Disturbances Following CCI and Polytrauma

Catwalk analysis was used to detect static and dynamic gait disturbances due to CCI alone (Additional Figure 1D–R). In contrast to the von Frey Results (Figure 1B and C), CCI-related gait changes remained modest or tracked closely with sham surgery controls. The most pronounced changes in CCI-affected hindlimbs were a tendency to increased swing time (Additional Figure 1E), decreased intermediate toe spread (Additional Figure 1F) and increased body speed variation [(%) Body speed / average speed] (Additional Figure 1G), with a spike in contralateral hindlimb single stance time 7 days post-injury (Additional Figure 1N). No significant differences were observed in stand time, stand index, print area, swing speed, stride length, step cycle time, body speed, average speed, dual stance time, regularity index or sciatic static index[44] compared to sham controls (Additional Figure 1D, H, I, J–M and O–R).

We previously showed severe 5 mm muscle contusion produces transient changes in stand and speed parameters.[18] Here, we show that 1 mm polytrauma (Figure 1G–L and Additional Figure 2A–E) and 3 mm polytrauma (Additional Figure 2F–O) also exhibit gait changes that are largely minor compared to control groups. Similar patterns in paw print analyses were observed in both polytrauma models. The most pronounced difference was an attenuated increase in print area in 1 mm polytrauma mice versus naïve controls (Figure 1I) and 3 mm polytrauma mice versus controls (Additional Figure 2L). Body speed variability showed a tendency to increase around 10 days post 1 mm polytrauma (Figure 1J) and a strong, consistent tendency towards increased speed variation in 3 mm polytrauma (Additional Figure 2M). This occurred despite only minor changes in body speed (Additional Figure 2N). As a positive control for gait changes, and consistent with prior reports,[36] we confirmed that robust, statistically significant changes in gait patterns were detectable in mice 14 days after spared nerve injury (SNI) surgery (Additional Figure 2P–E'), reaffirming that the degree of nerve injury surgery can influence the extent of gait changes.

NIRF Imaging of Macrophage Infiltration Following Nerve and Muscle Contusion

The role of macrophages in polytrauma was first examined by non-invasive imaging of their accumulation at the site of nerve and muscle contusion in the polytrauma model. As we have shown previously, macrophage infiltration can be imaged using nanoemulsions that carry two fluorescent dyes, a red fluorescent (DiI) and NIRF dye (DiR), enabling non-invasive, longitudinal tracking of macrophage accumulation by increased fluorescence at sites of injury.[30] In the polytrauma model, the NIRF signal was increased in all ipsilateral hindlimbs at 3 days post-injury (Figure 2A), when
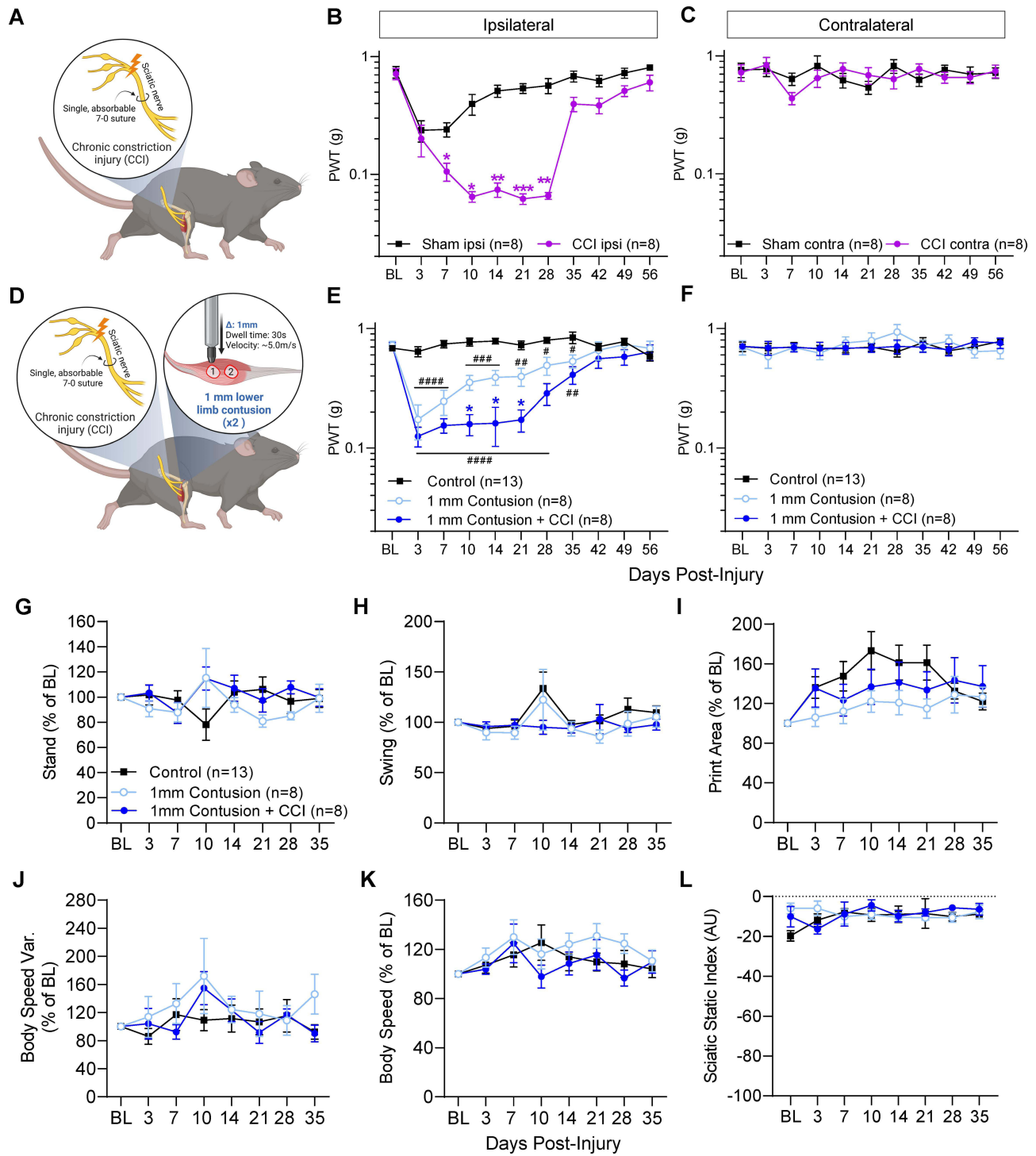
Figure 1 Mild sciatic nerve constriction and neuromuscular polytrauma model. (**A**) Illustration of mild chronic constriction injury (CCI), delivered by placing a single absorbable ligature around the sciatic nerve. (**B**) CCI causes significant von Frey hypersensitivity from 7–28 days post-injury, before largely reversing from 35 days onwards. (**C**) Hindpaws contralateral to CCI surgery show no significant changes in sensitivity across time. Group "n" reported in parentheses in legend; n=3 males, 5 females per group. Mean ± SEM, */**/*** p=<0.05, 0.01, 0.001 "Sham Ipsi" versus "CCI Ipsi" at respective timepoints, two-way repeated measures ANOVA, Šídák's multiple comparisons test. (**D**) Illustration of mild CCI paired with 1 mm lower limb contusion ("1 mm polytrauma"). (**E**) Uninjured control mice show stable von Frey sensitivity. "1 mm contusion" results in significant hypersensitivity versus control mice up to 35 days post-injury (mice in this group also received sham CCI surgery to control for skin and muscle incision). Pairing 1 mm contusion with mild CCI ("1 mm contusion + CCI") resulted in significantly greater hypersensitivity at 10, 14 and 21 days post-injury. (**F**) Hindpaws contralateral to contusion/CCI show no significant changes in sensitivity across time. Group "n" reported in parentheses in legends; n=5 males, 3 females (per contusion ± CCI group); n=8 males, 5 females (naïve control group). * p=<0.05 "contusion" versus "contusion + CCI". Mean ± SEM, #/##/###/#### p=<0.05, 0.01, 0.001, 0.0001 versus "control" at respective timepoints, two-way repeated measures ANOVA, Šídák's multiple comparisons test. (**G–L**) All control, contusion and contusion + CCI values ipsilateral to injury are depicted as percent of baseline (BL) readings. (**G**) Stand time. (**H**) Swing time. (**I**) Print area. (**J**) Body speed variability. (**K**) Body speed. (**L**) Sciatic static index. Group "n" reported in parentheses in legends; n=5 males, 3 females (per contusion ± CCI group); n=8 males, 5 females (naïve control group). Additional gait metrics are described in Additional File 1 and depicted in Additional Figure 2.

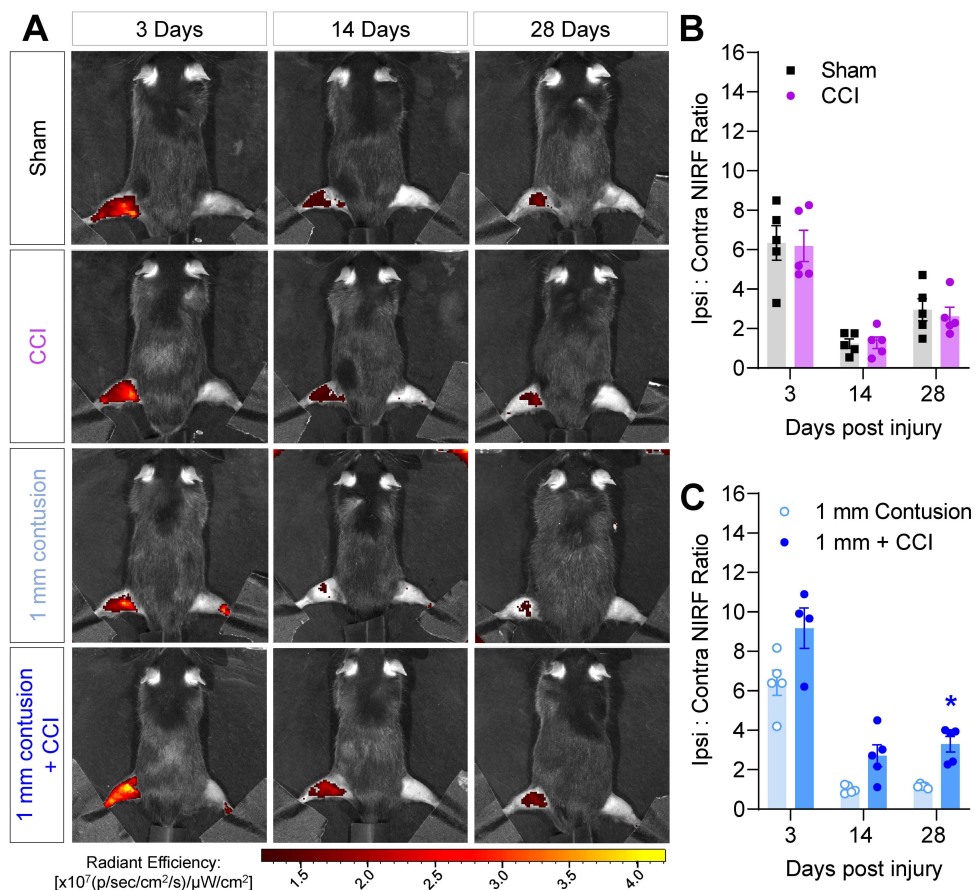**Figure 2** NIRF imaging of macrophage-targeted nanoemulsions detects acute macrophage accumulation following polytrauma. (**A**) 24h prior to injury of the left hindlimb, mice received DF-NE to track macrophage accumulation non-invasively. Representative NIRF images of mice 3 days (left column), 14 days (center column) and 28 days (right column) post-injury. Top row: Sham surgery. Second row: CCI only. Third row: 1 mm contusion only. Bottom row: 1 mm polytrauma. (**B** and **C**) Quantification of hindlimb NIRF signal across time for each injury group. Values are expressed as the ratio of ipsilateral: contralateral fluorescence. N= 3 males, 2 females per group. Mean ± SEM, *=$p < 0.05$ versus "1 mm contusion". Two-way repeat measures ANOVA, Šídák's multiple comparisons test.

compared to contralateral hindlimbs used as an internal control. No significant differences were observed between sham surgery and CCI groups (Figure 2B), but a persistent elevation in NIRF signal was detected in 1 mm contusion + CCI animals versus contusion alone, which was statistically significant at 28 days post-injury (Figure 2C).

Polytrauma-Induced Macrophage Accumulation

Increased macrophage infiltration in peripheral nerves has been observed in CCI models.[45] In this study, a mild CCI produced sustained macrophage accumulation in ipsilateral sciatic nerves (Additional Figure 3A), peaking at 14 days post-injury compared to sham controls (Additional Figure 3B). Consistent with previous studies, the single, loose ligature elevated macrophage density in sciatic nerve concomitantly with pain hypersensitivity. Since NIRF imaging showed more sustained macrophage accumulation in polytrauma mice prolonged timepoints, we next wanted to determine in which tissues macrophage accumulation differed between 1 mm contusion and 1 mm polytrauma. Significant macrophage infiltration was observed in 1 mm polytrauma dermis at 3 days post-injury (Figure 3A and B and Additional Figure 4A). This polytrauma-related increase persisted in the underlying biceps femoris muscle until day 14 (Figure 3C, D and Additional Figure 4B). Although the trend toward an acute increase was directionally similar in the gastrocnemius muscle, polytrauma macrophage density was not significantly greater in this muscle group (Figure 3E, F and Additional Figure 4C).
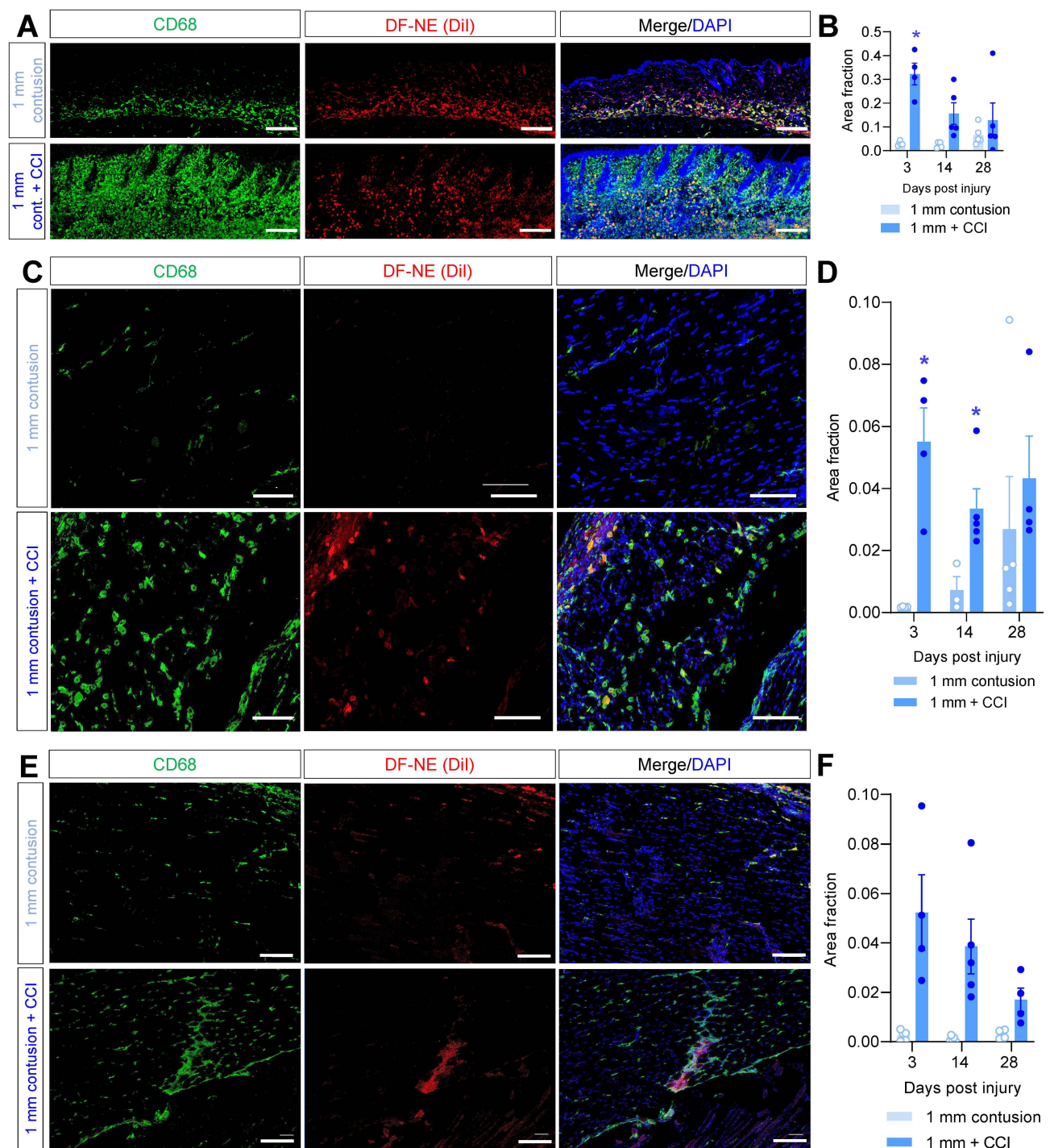
Figure 3 Acutely increased macrophage density in dermis and lower limb muscles of polytrauma mice. Skin samples collected from the site of lower limb contusion were fixed and processed for immunostaining. (**A**) Pan-macrophage marker CD68 (green) shows widespread colocalization with DiI fluorescence (red), indicative of DF-NE uptake (dual labeled with DiI and DiR). DAPI: blue. Top row represents 1 mm contusion skin 3d post-injury, bottom row represents 1 mm polytrauma 3d post-injury. Scale bar: 0.2 mm. (**B**) Quantification of skin CD68 density shows a significant increase in ipsilateral skin subjected to 1 mm polytrauma versus contusion alone at 3d post-injury. (**C**) Biceps femoris muscle samples show sparse staining in 1 mm contusion only (top row). DAPI: blue. Bottom row shows greater density of CD68 fluorescence and DiI signal in 1 mm polytrauma group at the same time point. Scale bar: 0.1 mm. (**D**) Quantification of CD68 density shows a significant increase in ipsilateral biceps femoris subjected to 1 mm polytrauma versus contusion alone at 3d and 14d post-injury. (**E**) Gastrocnemius muscle samples show sparse staining in 1 mm contusion only (top row). DAPI: blue. Bottom row shows a modest increase in CD68 fluorescence and DiI signal in 1 mm polytrauma group at the same time point. Scale bar: 0.1 mm. (**F**) Quantification of CD68 density shows a statistically non-significant but strong tendency toward an increase in ipsilateral gastrocnemius subjected to 1 mm polytrauma versus contusion alone at 3d and 14d post-injury. * = p <0.05 1mm contusion versus 1 mm polytrauma, two-way ANOVA, Šídák's multiple comparisons test (Representative images for 3, 14 and 28d post-injury are shown in Additional Figure 4A–C).

Persistent Macrophage Accumulation in Polytrauma Sciatic Nerve is Required to Maintain Pain

In mice subjected to CCI alone, sciatic nerve macrophage density peaks concomitantly with pain hypersensitivity at 14d post-injury (Additional Figure 3). We also reported a modest but persistent increase in sciatic nerve macrophage density following muscle contusion alone.[18] Now combining these injuries in our polytrauma model, we observed more sustained macrophage infiltration of the sciatic nerve (Figure 4A and B), indicating prolonged macrophage presence in the injured sciatic nerve. Macrophage density was significantly greater in mice that underwent 1 mm polytrauma versus 1 mm contusion alone, and importantly, the elevation in macrophage density persisted at 28 days, on contrast to CCI alone. In order to test the necessity of macrophage accumulation for the pain hypersensitivity associated with polytrauma, we used a chemogenetic ablation approach in macrophage Fas-induced apoptosis (MaFIA) mice,[16,38] to induce peripheral macrophage apoptosis. MaFIA mice develop polytrauma-associated pain hypersensitivity to the same extent as wild-type mice at 3- and 7 days post-injury (Figure 4C). Following chemogenetic ablation on days 7–9 post-injury, pain hypersensitivity was normalized and mice were significantly less sensitive than vehicle-treated controls until 21d post-injury, after which time vehicle-treated mice begin to recover as usual. Contralateral hindlimbs were unaffected by macrophage ablation (Additional Figure 5A), and the effect was similar between males and females (Additional Figure 5B–E).
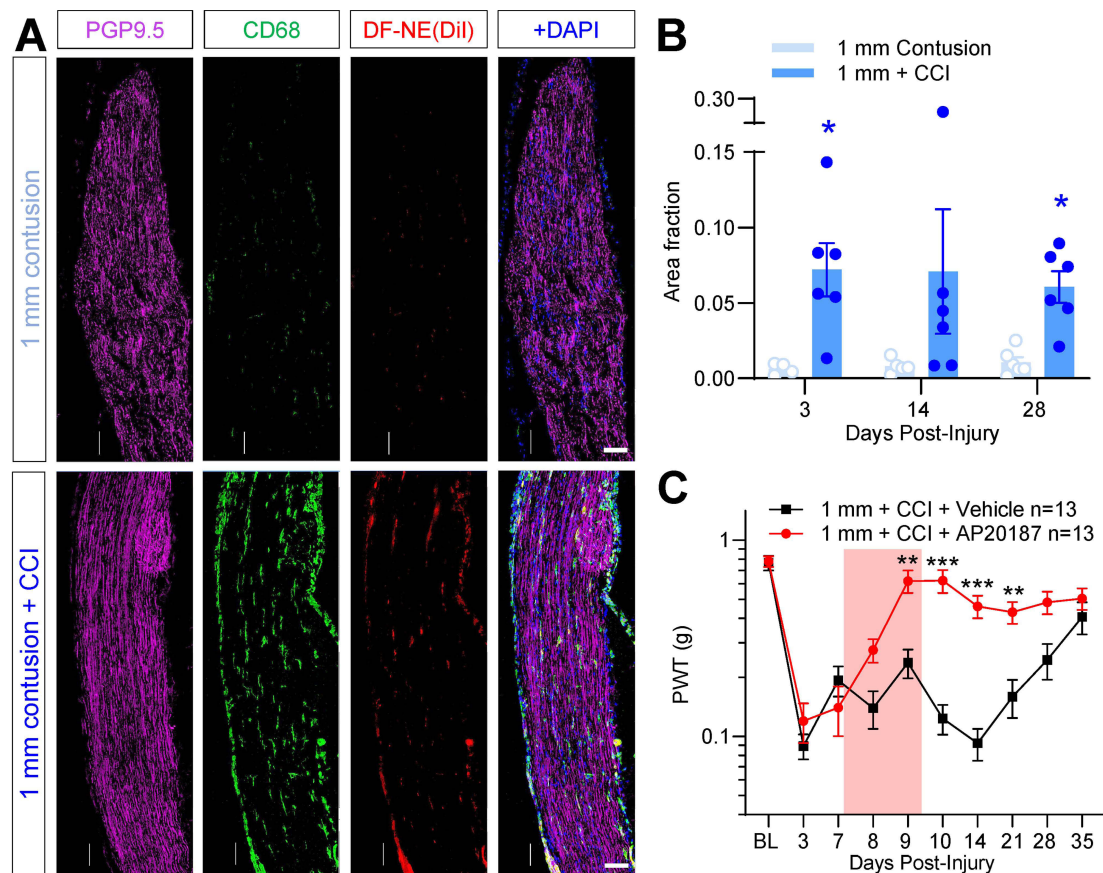

Figure 4 Sustained accumulation of macrophages in sciatic nerves of mice subjected to polytrauma. Sciatic nerves collected from the lower limb contusion were fixed and processed for immunostaining 28 days post-injury. (**A**) Pan-macrophage marker CD68 (green) and DiI fluorescence (red) show sparse staining in 1 mm contusion only (top row). PGP9.5: Magenta. DAPI: blue. Bottom row shows a modest increase in CD68 fluorescence and DiI signal in 1 mm polytrauma group at the same time point. Scale bar: 0.1 mm. (**B**) Quantification of CD68 density shows a significant increase in ipsilateral sciatic subjected to 1 mm polytrauma versus contusion alone at 3d and 28d post-injury. * = p <0.05 1mm contusion versus 1 mm polytrauma, two-way ANOVA, Šídák's multiple comparisons test. (**C**) MaFIA mice subjected to 1 mm polytrauma behave similar to wild-type C57BL/6 mice in the acute stages post-injury. AP20187 treatment (3 days, 2 mg/kg, i.p., red box) durably reversed pain hypersensitivity in these mice without affecting contralateral hindpaw sensitivity (Additional Figure 5A). **/*** = p <0.01, 0.001, 1mm polytrauma + vehicle versus 1 mm polytrauma + AP20187, two-way ANOVA, Šídák's multiple comparisons test.

COX-2 Inhibitor Loaded NIRF Labeled Nanoemulsions for Macrophage Modulation

In order to test whether macrophages at the sites of nerve injury and muscle contusion play a direct role in muscle and nerve inflammation, we and others have used macrophage-targeted approaches to modify macrophage activity and assess the effect on pain sensitivity.[27–31] Persistent macrophage activation results in overexpression of COX-2, which is a rate-limiting enzyme for prostaglandin E2 (PGE$_2$) synthesis. For this study, we loaded the COX-2 inhibitor celecoxib into a nanoemulsion (CXB-NE) to suppress macrophage-driven PGE$_2$ synthesis and proinflammatory mediator release. Our previously reported CXB-NE,[41] composed of perfluorocarbon, hydrocarbon, and surfactants with low droplet size (~130 nm, Figure 5A), was re-formulated for this study. The drug-free nanoemulsion (DF-NE) control, of the same composition without the presence of drug, is used as a negative control and a macrophage-specific imaging agent. Both nanoemulsions allow for tracking macrophages in vivo and ex vivo as they contain two dyes: DiI, in support of fluorescence microscopy in isolated tissues, and DiR, for live NIRF imaging. Figure 5 summarizes the in vitro characterization of CXB-NE and DF-NE used in this study. Both the NEs were taken up by macrophages within 3 hours of exposure as determined by flow cytometry (Figure 5B). Macrophage uptake was also demonstrated qualitatively by fluorescent microscopy (Figure 5C). CXB-NE treatment also inhibited PGE$_2$ release from activated macrophages in vitro[41] and in vivo,[27,28] and was also able to suppress the release of proinflammatory cytokines TNF-α and IL-6 from activated macrophages in vitro.[41] Therefore, we chose CXB-NE to modulate macrophages in the polytrauma model in this study.
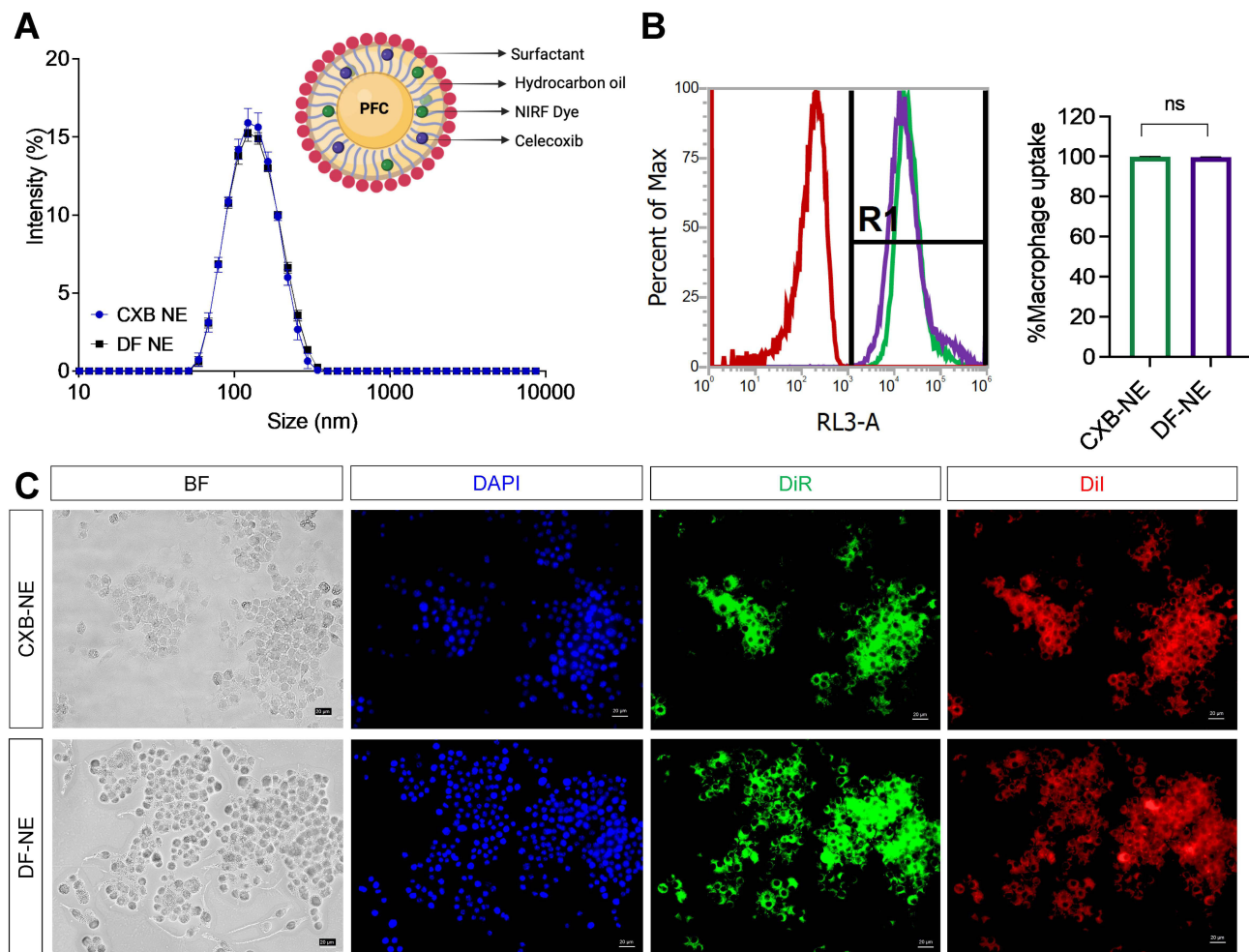

Figure 5 Characterization of CXB-NE and DF-NE. (**A**) Overlay of average size distribution by intensity between CXB-NE and DF-NE with pictorial representation of CXB-NE droplet. (**B**) Macrophage uptake of CXB-NE and DF-NE quantified by flow cytometry. R1: DiR+ macrophages. The data is shown as the mean ± SD (n = 3/group), and 50,000 cells were counted. (**C**) Fluorescence images of RAW 264.7 macrophages after 24 h labeling with CXB-NE and DF-NE.

Macrophage-Specific COX-2 Inhibition Prevents Sustained Pain Following Polytrauma

To test whether modifying macrophage activity could influence polytrauma pain behavior, we used CXB-NE to shut down COX-2 driven prostaglandin production specifically in injury-infiltrating macrophages (Figure 6A). We administered CXB-NE to treatment groups, and DF-NE to controls in mice subjected to 1 mm polytrauma 7 days post-injury (Figure 6B and C). Uninjured male controls that received CXB-NE show stable von Frey sensitivity and, as expected, 1 mm polytrauma males injected with DF-NE 7 days post-injury showed unaltered progression of pain hypersensitivity, comparable to that seen in un-injected mice (Figure 6B). Injured males that received CXB-NE, showed a progressive normalization of sensitivity which reached significance from 14 to 35 days post-injury. However, female mice that received CXB-NE 7 days post-injury did not show any significant reduction in hypersensitivity (Figure 6C). Contralateral hindpaw thresholds for all groups in both sexes were unaffected by DF-NE or CXB-NE (Additional Figure 6A).

We next determined if dosing more acutely post-injury affected the anti-hyperalgesic efficacy of CXB-NE (Figure 7A). When male mice received CXB-NE at 3 days post-injury, a more pronounced and statistically significant anti-hyperalgesia was observed versus DF-NE controls (Figure 7B). Interestingly, delivering two doses of CXB-NE at 24 and 72h post-injury also significantly reversed hypersensitivity in male mice (Figure 7C and D), though it did not outperform a single dose of CXB-NE at 3d alone. No significant changes were seen in von Frey thresholds in the contralateral hindpaws of these mice (Additional Figure 6B and C). Despite significant pain relief in these mice, it was not associated with a significant improvement in grip strength (Additional Figure 6D). Similar to female mice dosed at 7 days post-injury, female mice that received CXB-NE at 24 and 72 h showed only a slight, non-significant tendency toward reduced hypersensitivity (Figure 6D), indicating that the more limited efficacy of CXB-NE in female mice is similar across intervention time points.
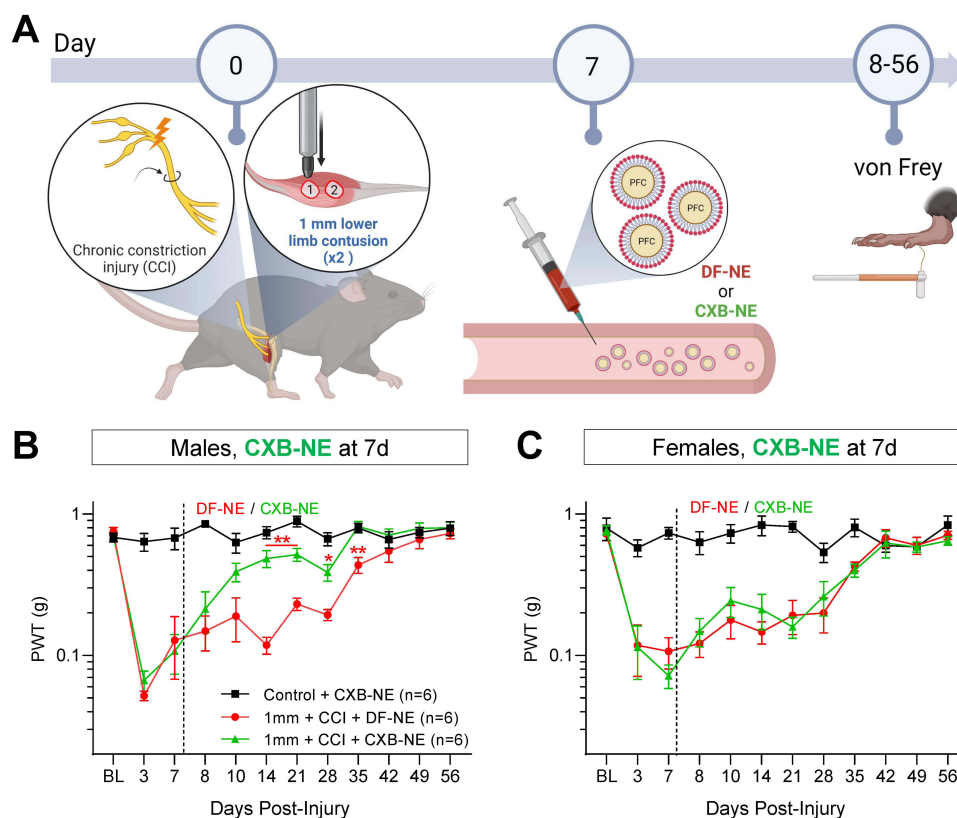

Figure 6 CXB-NE reduces hypersensitivity when delivered 7 days post-injury in male mice. (**A**) Illustration depicting timeline of injury, behavioral testing and delivery of DF-NE or CXB-NE (0.2 mL, i.v.) 7 days post-injury. (**B**) Naïve control males treated with CXB-NE show stable von Frey withdrawal thresholds. Three- and 7-days post-injury, 1 mm polytrauma groups show reduced thresholds. After testing von Frey on day 7 post-injury, groups received either i.v. DF-NE or CXB-NE. Mice treated with CXB-NE showed a gradual yet persistent recovery of sensitivity, becoming significantly reversed compared to DF-NE controls from 14 to 35 days post-injury. (**C**) In contrast, an identical experiment in females did not show reversal of hypersensitivity with CXB-NE. */** p=<0.05/0.01 "1mm polytrauma + DF-NE" versus "1mm polytrauma + CXB-NE". Two-way, repeat measures ANOVA, Šídák's multiple comparisons test.
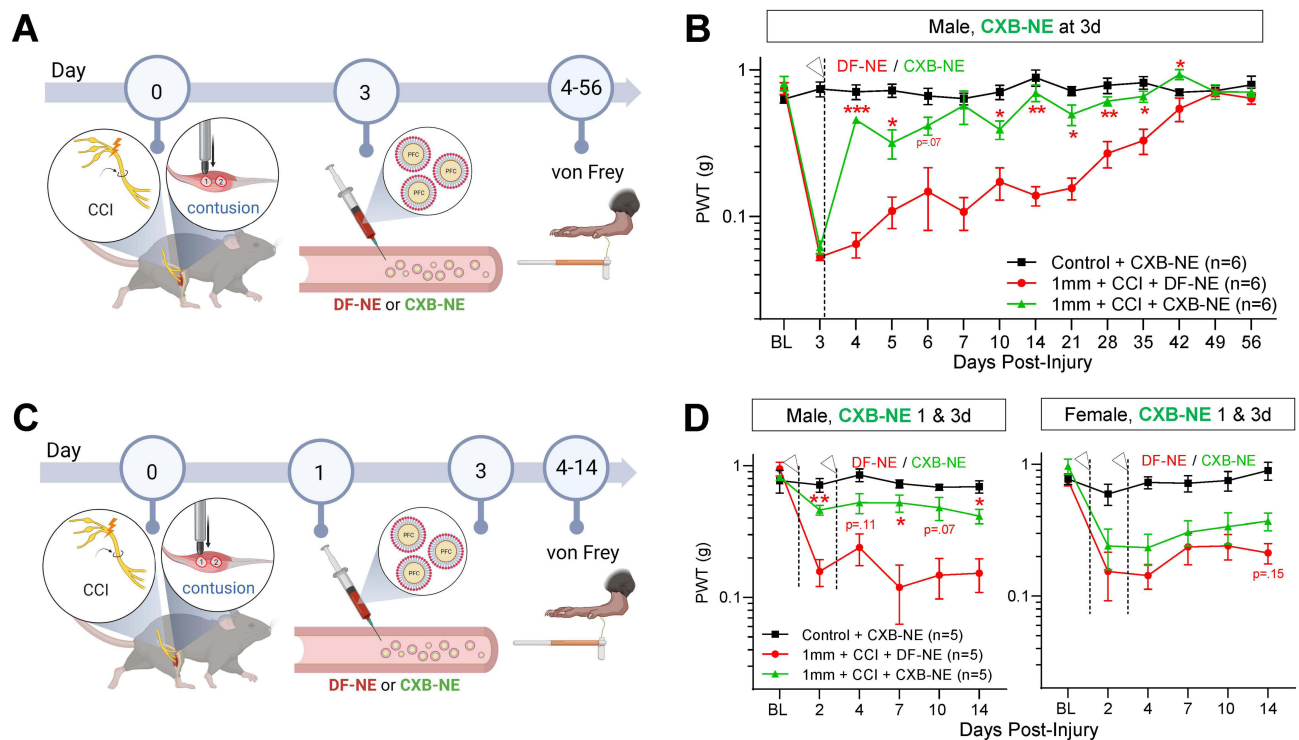
Figure 7 CXB-NE reduces hypersensitivity in the acute post-injury window in male mice. (**A**) Illustration depicting timeline of injury, behavioral testing and delivery of DF-NE or CXB-NE (0.2 mL, i.v.) in two treatment paradigms, either 3 days post-injury or 1 day and 3 days post-injury. (**B**) Naïve control males treated with CXB-NE show stable von Frey withdrawal thresholds. Post-injury, 1 mm polytrauma groups show the expected hypersensitivity. After testing von Frey on day 3 post-injury, groups received either i.v. DF-NE or CXB-NE. Mice treated with CXB-NE showed a significant and sustained attenuation of sensitivity, becoming significantly reversed compared to DF-NE controls at 4 and 5 days post-injury and from 10–42 days post-injury. (**C**) Male mice were subjected to polytrauma injury and treated with DF-NE or CXB-NE 24h and 72h after injury. This additional dosing did not further improve the CXB-NE-mediated attenuation of hypersensitivity. (**D**) In contrast, an identical experiment in females did not show statistically significant reversal of hypersensitivity with CXB-NE. */**/*** p=<0.05/0.01/0.001 "1 mm polytrauma + DF-NE" versus "1 mm polytrauma + CXB-NE". Two-way, repeat measures ANOVA, Šídák's multiple comparisons test.

Previous studies using NIRF imaging also showed CXB-NE and DF-NE accumulated at sites of inflammation.[28,30,32] In this study, both nanoemulsions are labeled with the same fluorescent dyes (DiI and DiR) at the same concentration, which facilitated further NIRF imaging and tissue analyses. Using the groups of male and female polytrauma mice that were dosed at 24h and 72h after injury, we carried out NIRF imaging at 2, 4, 7- and 10 days post-injury. Male mice treated with CXB-NE showed a significant reduction in macrophage density 24 hours after initial injection versus DF-NE controls (Figure 8A and C). NIRF imaging on days 4, 7 and 10 showed a persistent trend toward a reduced NIRF ratio in CXB-NE-injected males versus their DF-NE-injected counterparts (Figure 8C). However, CXB-NE was not associated with reduced NIRF signal versus DF-NE controls in females (Figure 8B and D).

CXB-NE Reduces Inflammatory Mediator Output in the Acute Post-Injury Window

We reasoned that acute pain relief induced by CXB-NE may be induced by a reduction in macrophage COX-2 activity, reducing production of pro-nociceptive inflammatory mediators. Using male mice, we analyzed the cytokine content of ipsilateral and contralateral polytrauma sciatic nerves 24 h after treatment with DF-NE or CXB-NE, and 48 h after injury. Of the 111 factors screened, 60 showed a 2-fold or greater upregulation and 7 showed a 2-fold or greater downregulation in DF-NE ipsilateral versus contralateral nerves and were selected for further analysis (Figure 8E and Additional Table 1). After adjusting for multiple comparisons, 13 factors were significantly (p=<0.05) downregulated by CXB-NE treatment. Among these reduced factors were pro-inflammatory proteases and adhesion molecules, such as MMP-3 and MMP-9[46] and reduced monocyte chemoattractants, such as CCL2. CXB-NE also reduced expression of factors associated with M1-like macrophage polarization, such as Lipocalin-2[47,48] and enhanced expression of leptin, which can promote M2 macrophage polarization.[49] The factors that were either elevated in CXB-NE mice or reduced in DF-NE-treated mice were not significantly different from each other (Additional Figure 7A and B). Collectively, this indicates
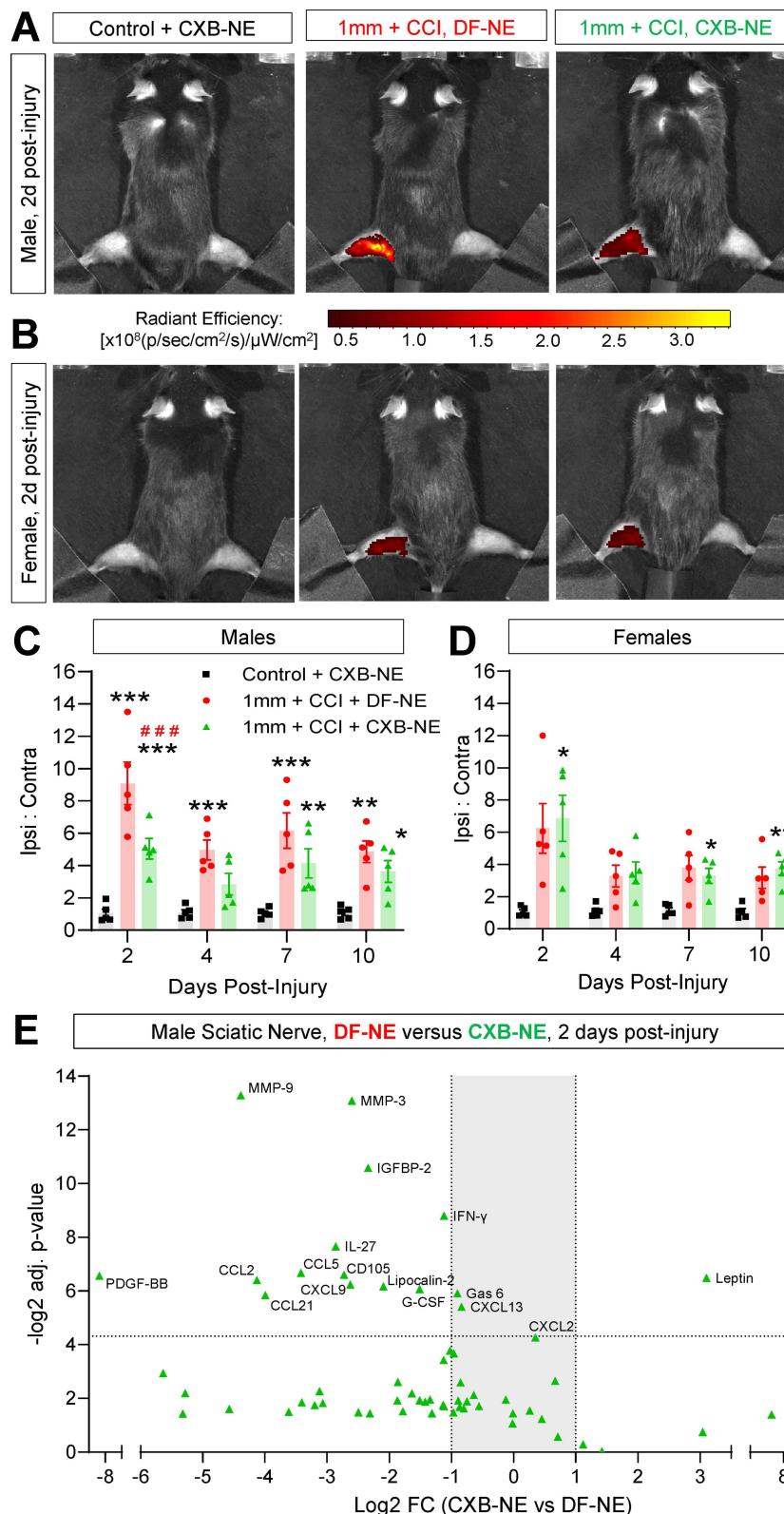
Figure 8 CXB-NE reduces NIRF signal and inflammation in the acute post-injury window in male mice. (**A**) Representative images of male mice 2 days post-injury and 24h post-dosing with DF-NE or CXB-NE (0.2 mL, i.v.). (**B**) Quantification of ipsilateral to contralateral NIRF ratio shows a significant increase versus control at all time points. 2 days post-injury, polytrauma mice that received CXB-NE show significantly less NIRF signal than their DF-NE-injected counterparts, a trend that persists at days 4, 7 and 10 post-injury. These effects of CXB-NE were not observed in female mice (**C** and **D**). */**/*** $p=<0.05/0.01/0.001$ "1 mm polytrauma + DF-NE" versus "1 mm polytrauma + CXB-NE". Two-way, repeat measures ANOVA, Šídák's multiple comparisons test. (**E**) Two days post-polytrauma, and 24h after dosing with DF-NE or CXB-NE in male mice, (0.2 mL, i.v.), sciatic nerves were homogenized and probed semi-quantitatively for cytokine/chemokine content. Detected factors with ≥2-fold expression in ipsilateral versus contralateral nerves from DF-NE mice are shown plotted by significance level (adjusted p-value) on the y-axis (FDR 0.05). Fold-change of all factors detected are listed in Additional File 1.

that pain relief following CXB-NE injection is associated with anti-inflammatory activity in macrophages within the sciatic nerve.

Discussion

The primary goals of this study were to use our recently developed lower limb contusion model to determine the impact of nerve damage and neuroinflammation on healing from complex polytrauma injuries, an approach that is intended to more closely reflect the nature of traumatic injuries that often develop into chronic pain.[50] We previously showed that lower-limb impacts of sub-maximal intensity showed persistent accumulation of macrophages in the ipsilateral sciatic nerve.[18] Macrophages are crucial drivers of pain and are also valuable for bringing about its resolution.[16,40,51] Macrophage infiltration of nerves and sensory ganglia is typically a feature of neuropathic pain states. Such infiltration is known to drive pathophysiological changes to nerve function.[14,15] Indeed, prior studies have demonstrated that compromised innervation (whether by targeted ablation or disease) can delay wound healing.[12,13] The purpose of this study was therefore two-fold: to determine the extent to which introducing nerve injury would augment pain and compromise healing due to muscle contusion and establish if macrophage nanoimmunomodulation (CXB-NE) could accelerate recovery by modifying the inflammatory output in the injured nerve.

Others have shown previously that chronic constriction injury causes ectopic discharge and co-existence of degenerating and spared axons in the target tissues. It is thought that inflammation initiated by injured fibers causes hypersensitivity in the remaining uninjured fibers, triggering spontaneous activity and pain behaviors.[52] We found that adding a mild version of CCI to lower limb contusion extended the duration of hypersensitivity in the von Frey assay. Interestingly, the elevation in macrophage content of CCI sciatic nerves returned to near-normal levels at 28 days, while macrophage density was still significantly elevated at this timepoint after polytrauma. Interestingly, peak hypersensitivity in the von Frey assay was somewhat greater in controls that received nerve constriction alone versus constriction/contusion "polytrauma". While it is possible that injury of lower limb muscles reduces the ability of the hind paw to reflexively withdraw from stimulation, this seems unlikely given the lack of overt disturbances to gait in these mice. Alternatively, generating two anatomically distinct sites of injury may be an example of "pain inhibiting pain", also known as conditioned pain modulation.[53] This is a phenomenon driven by engagement of descending inhibitory controls at the level of the spinal cord.[54] Coupled with the impaired resolution of inflammation due to sensory nerve damage, this inhibitory control may explain the distinct behavioral responses observed in polytrauma mice.

Consistent with our prior data in muscle contusion alone,[18] we did not detect widespread, sustained changes to gait metrics, apart from an attenuation of the increase in print area and a trend toward increased body speed variability with the more severe 3mm contusion. The change in uninjured mouse gait patterns over time is likely due to conditioning to repeat testing in the assay, others have reported similar findings.[55] This lack of overt disruption of gait following injury contrasts with models of deafferentation, such as SNI, where we detect widespread gait deficits.[36] Rodent models with a crushed sciatic nerve injury exhibit dysfunctions in paw placement metrics such as contact intensity and print area with changes to gait parameters such as swing duration and stance.[56] In a similar model to the one used in this study, mechanical pain from chronic constriction of the sciatic nerve correlated with paw print intensity and gait metrics like swing and stance duration,[57] though it is important to note that the CCI we employed in this study used a single suture and therefore introduces a less severe injury. Importantly, prior studies suggest that the major gait deficits detected in SNI mice are not reversible with analgesics[36] – perhaps suggesting that in this model pain-related changes are either too minimal or variable to detect reliably.

As we previously reported in muscle contusion alone, we see an acute increase in macrophage density in contused tissues within 3 days of injury that diminishes rapidly. However, concomitant nerve constriction prolonged this elevated macrophage density in the dermis, lower leg muscles and sciatic nerve.[58] There is a requirement for the ongoing presence of macrophages in maintaining pain hypersensitivity, since inducible ablation of macrophages brought about sustained recovery from pain.[16,59] Previous work has shown that ablation of macrophages can reverse pain hypersensitivity, though this was done in SNI mice, wherein tactile and cold hypersensitivity returned once macrophages re-populated the site of injury.[16,17] Further work is needed to determine the ways in which nerve-resident macrophages differ pre- and post-ablation, both phenotypically and functionally.

Because inducing macrophage apoptosis 7–9 days post-injury attenuated pain hypersensitivity, we next wanted to establish if modifying macrophage function with the COX-2 inhibitor celecoxib would also be effective. Nanoemulsions loaded with celecoxib showed a modest effect when delivered 7 days post-injury, but only in male mice. Intervening earlier had a more significant effect, suggesting that inhibiting COX-2 in macrophages is more effective in the acute phase post-injury (within 72h). Assuming modifying macrophage activity has downstream effects on axonal excitability, this acute window of opportunity would be consistent with timing of nerve blocks being effective. Nerve blocks are typically the most effective within the first 3–5 days following injury, with their effectiveness diminishing as neuropathic pain becomes more established (ie 10 days post-injury and beyond).[60]

Prior studies have shown in more severe CCI injury that CXB-NE can relieve pain hypersensitivity. As reported here, a single dose of CXB-NE, delivering a dose of celecoxib orders of magnitude lower than a conventional systemic dose was able to relieve pain. However, in prior reports this pain relief was transient (3–5 days of pain relief) and hypersensitivity eventually returned to the injured hindlimb.[27,61] Since those studies used the more severe CCI model, this may suggest that durable reversal or transient relief could be determined by the severity of injury. Perhaps more severe injuries eventually exhaust CXB-NE-suppressed macrophages and would require repeat CXB-NE dosing. Further work is required to understand the mechanisms underlying these differences.

The striking sex differences in the efficacy of CXB-NE add to the body of evidence that chronic pain tends to be more macrophage-dependent in males than in females.[62] These data are broadly consistent with prior reports of CXB-NE efficacy in more conventional CCI.[31] The observation that macrophage ablation attenuates hypersensitivity in both sexes is consistent with our prior data in the spared nerve injury model.[16] Taken in concert with the CXB-NE data, this may suggest a sex difference in macrophage dependence on COX-2 activity, rather than macrophages being entirely dispensable for polytrauma pain in females per se. The inability of CXB-NE to reduce macrophage NIRF signal in females would also be consistent with macrophage accumulation in females being less dependent on processes driven by COX-2 metabolites, such as PGE_2. Within 24 hours of dosing polytrauma males with CXB-NE, we see suppression of inflammatory cytokines, many of which have a known role in driving pro-inflammatory or inhibiting anti-inflammatory macrophage polarization. The acute differences in expression of these cytokines suggest a model in which the anti-inflammatory activity of CXB-NE precedes and/or initiates a net anti-inflammatory shift in macrophage polarization to promote lasting healing.

Conclusion

Our neuromuscular polytrauma model is distinct from neuronal injury or soft tissue contusion alone, both in terms of pain-related behaviors and innate inflammation. The augmented macrophage infiltration in polytrauma is required for maintenance of pain hypersensitivity. Crucially, attenuation of this pain by delivery of macrophage-targeted inhibition of COX-2 was more effective in male mice than female mice.

Abbreviations

ANOVA, Analysis of variance; BL, Baseline; cm^2, Centimeter squared; CCI, Chronic constriction injury; CFA, Complete Freund's adjuvant; COX-2, Cyclooxygenase-2; CXB-NE, Celecoxib nanoemulsion; DAPI, 4′,6-diamidino-2-phenylindole; DF-NE, drug-free nanoemulsion; DiI, 1.1'-dioctadecyl-3,3,3'3'-tetramethylindocarbocyanine perchlorate; DiR, 1.1'-dioctadecyl -3,3,3',3'-tetramethylindotricarbocyanine iodide; DMSO, Dimethyl sulfoxide; DRG, Dorsal root ganglion/ganglia; EGF, Epidermal growth factor; G, Grams; IVIS, In vivo Imaging System; µW, Microwatt; MaFIA, Macrophage Fas-induced apoptosis; MMP-9, Matrix metalloprotease-9; NE, Nanoemulsion; nm, nanometer; NIRF, Near-infrared fluorescence; NSAID, Non-steroidal anti-inflammatory drug; P, Photons; PBS, Phosphate-buffered saline; PFA, Paraformaldehyde; PGE_2, Prostaglandin E2; PWT, Paw withdrawal threshold; RT, Room temperature; SNI, Spared nerve injury.

Acknowledgments

resource supported by the NIH/NCI under award number P30CA016672. We wish to thank Kiersten Maldonado, Vivien Van and Angela M. Casaril for technical assistance.

Disclosure

The authors report no conflicts of interest in this work.

References

1. Hurtgen BJ, Ward CL, Garg K, et al. Severe muscle trauma triggers heightened and prolonged local musculoskeletal inflammation and impairs adjacent tibia fracture healing. *J Musculoskelet Neuronal Interact*. 2016;16:122–134.
2. Kim H, Wang SY, Kwak G, et al. Exosome-guided phenotypic switch of M1 to M2 macrophages for cutaneous wound healing. *Advan Sci*. 2019;6:1900513. doi:10.1002/advs.201900513
3. Porcuna J, Menendez-Gutierrez MP, Ricote M. Molecular control of tissue-resident macrophage identity by nuclear receptors. *Curr Opin Pharmacol*. 2020;53:27–34. doi:10.1016/j.coph.2020.04.001
4. Wofford KL, Shultz RB, Burrell JC, Cullen DK. Neuroimmune interactions and immunoengineering strategies in peripheral nerve repair. *Progr Neurobiol*. 2022;208:102172. doi:10.1016/j.pneurobio.2021.102172
5. Fiore NT, Debs SR, Hayes JP, Duffy SS, Moalem-Taylor G. Pain-resolving immune mechanisms in neuropathic pain. *Nat Rev Neurol*. 2023;19:199–220. doi:10.1038/s41582-023-00777-3
6. Tanaka T, Okuda H, Isonishi A, et al. Dermal macrophages set pain sensitivity by modulating the amount of tissue NGF through an SNX25-Nrf2 pathway. *Nat Immunol*. 2023;24:439–451. doi:10.1038/s41590-022-01418-5
7. Stratos I, Graff J, Rotter R, Mittlmeier T, Vollmar B. Open blunt crush injury of different severity determines nature and extent of local tissue regeneration and repair. *J Orthop Res*. 2010;28:950–957. doi:10.1002/jor.21063
8. Tidball JG. Regulation of muscle growth and regeneration by the immune system. *Nat Rev Immunol*. 2017;17:165–178. doi:10.1038/nri.2016.150
9. Crisco JJ, Jokl P, Heinen GT, Connell MD, Panjabi MM. A muscle contusion injury model. Biomechanics, physiology, and histology. *Am J Sports Med*. 1994;22:702–710. doi:10.1177/036354659402200521
10. Rogeri PS, Gasparini SO, Martins GL, et al. Crosstalk between skeletal muscle and immune system: which roles do IL-6 and glutamine play? *Front Physiol*. 2020;11:582258. doi:10.3389/fphys.2020.582258
11. Leibovich H, Buzaglo N, Tsuriel S, et al. Abnormal reinnervation of denervated areas following nerve injury facilitates neuropathic pain. *Cells*. 2020;9:1007. doi:10.3390/cells9041007
12. Nowak NC, Menichella DM, Miller R, Paller AS. Cutaneous innervation in impaired diabetic wound healing. *Transl Res*. 2021;236:87–108. doi:10.1016/j.trsl.2021.05.003
13. Lu L, Liu D, Ying J, et al. Denervation affected skin wound healing in a modified rat model. *Int J Low Extrem Wounds*. 2022;2022:15347346221090758.
14. Zhang H, Li Y, de Carvalho-Barbosa M, et al. Dorsal root ganglion infiltration by macrophages contributes to paclitaxel chemotherapy-induced peripheral neuropathy. *J Pain*. 2016;17:775–786. doi:10.1016/j.jpain.2016.02.011
15. Old EA, Nadkarni S, Grist J, et al. Monocytes expressing CX3CR1 orchestrate the development of vincristine-induced pain. *J Clin Invest*. 2014;124:2023–2036. doi:10.1172/JCI71389
16. Shepherd AJ, Mickle AD, Golden JP, et al. Macrophage angiotensin II type 2 receptor triggers neuropathic pain. *Proc Natl Acad Sci USA*. 2018;115:E8057–E8066. doi:10.1073/pnas.1721815115
17. Shepherd AJ, Mohapatra DP. Attenuation of unevoked mechanical and cold pain hypersensitivities associated with experimental neuropathy in mice by angiotensin ii type-2 receptor antagonism. *Anesthesia Analg*. 2019;128:e84–e87. doi:10.1213/ANE.0000000000003857
18. Cortez I, Gaffney CM, Crelli CV, et al. Sustained pain and macrophage infiltration in a mouse muscle contusion model. *Muscle Nerve*. 2023;69:103–114. doi:10.1002/mus.28001
19. Corona BT, Rivera JC, Owens JG, Wenke JC, Rathbone CR. Volumetric muscle loss leads to permanent disability following extremity trauma. *J Rehabil Res Dev*. 2015;52:785–792. doi:10.1682/JRRD.2014.07.0165
20. Grimm PD, Mauntel TC, Potter BK. Combat and noncombat musculoskeletal injuries in the US military. *Sports Med Arthrosc Rev*. 2019;27:84–91. doi:10.1097/JSA.0000000000000246
21. Cross JD, Ficke JR, Hsu JR, Masini BD, Wenke JC. Battlefield orthopaedic injuries cause the majority of long-term disabilities. *J Am Acad Orthop Surg*. 2011;19 Suppl 1:S1–7. doi:10.5435/00124635-201102001-00002
22. Bennett GJ, Xie YK. A peripheral mononeuropathy in rat that produces disorders of pain sensation like those seen in man. *Pain*. 1988;33:87–107. doi:10.1016/0304-3959(88)90209-6
23. Wang Y, Zhang X, Guo Q-L, et al. Cyclooxygenase inhibitors suppress the expression of P2X(3) receptors in the DRG and attenuate hyperalgesia following chronic constriction injury in rats. *Neurosci Lett*. 2010;478:77–81. doi:10.1016/j.neulet.2010.04.069
24. Schafers M, Marziniak M, Sorkin LS, Yaksh TL, Sommer C. Cyclooxygenase inhibition in nerve-injury- and TNF-induced hyperalgesia in the rat. *Exp Neurol*. 2004;185:160–168. doi:10.1016/j.expneurol.2003.09.015
25. Grace PM, Hutchinson MR, Manavis J, Somogyi AA, Rolan PE. A novel animal model of graded neuropathic pain: utility to investigate mechanisms of population heterogeneity. *J Neurosci Methods*. 2010;193:47–53. doi:10.1016/j.jneumeth.2010.08.025
26. Ahamad N, Kar A, Mehta S, et al. Immunomodulatory nanosystems for treating inflammatory diseases. *Biomaterials*. 2021;274:120875. doi:10.1016/j.biomaterials.2021.120875
27. Saleem M, Deal B, Nehl E, Janjic JM, Pollock JA. Nanomedicine-driven neuropathic pain relief in a rat model is associated with macrophage polarity and mast cell activation. *Acta Neuropatholog Communic*. 2019;7:108. doi:10.1186/s40478-019-0762-y
28. Janjic JM, Vasudeva K, Saleem M, et al. Low-dose NSAIDs reduce pain via macrophage targeted nanoemulsion delivery to neuroinflammation of the sciatic nerve in rat. *J Neuroimmunol*. 2018;318:72–79. doi:10.1016/j.jneuroim.2018.02.010

29. Liu L, Karagoz H, Herneisey M, et al. Sex differences revealed in a mouse CFA inflammation model with macrophage targeted nanotheranostics. *Theranostics*. 2020;10:1694–1707. doi:10.7150/thno.41309

30. Nichols JM, Crelli CV, Liu L, et al. Tracking macrophages in diabetic neuropathy with two-color nanoemulsions for near-infrared fluorescent imaging and microscopy. *J Neuroinflammation*. 2021;18:299. doi:10.1186/s12974-021-02365-y

31. Deal B, Reynolds LM, Patterson C, Janjic JM, Pollock JA. Behavioral and inflammatory sex differences revealed by celecoxib nanotherapeutic treatment of peripheral neuroinflammation. *Sci Rep*. 2022;12:8472. doi:10.1038/s41598-022-12248-8

32. Patel SK, Beaino W, Anderson CJ, Janjic JM. Theranostic nanoemulsions for macrophage COX-2 inhibition in a murine inflammation model. *Clin Immunol*. 2015;160:59–70. doi:10.1016/j.clim.2015.04.019

33. Bindu S, Mazumder S, Bandyopadhyay U. Non-steroidal anti-inflammatory drugs (NSAIDs) and organ damage: a current perspective. *Biochem Pharmacol*. 2020;180:114147. doi:10.1016/j.bcp.2020.114147

34. Dobek GL, Fulkerson ND, Nicholas J, Schneider BS. Mouse model of muscle crush injury of the legs. *Comp Med*. 2013;63:227–232.

35. Chaplan SR, Bach FW, Pogrel JW, Chung JM, Yaksh TL. Quantitative assessment of tactile allodynia in the rat paw. *J Neurosci Meth*. 1994;53:55–63. doi:10.1016/0165-0270(94)90144-9

36. Shepherd AJ, Mohapatra DP. Pharmacological validation of voluntary gait and mechanical sensitivity assays associated with inflammatory and neuropathic pain in mice. *Neuropharmacology*. 2018;130:18–29. doi:10.1016/j.neuropharm.2017.11.036

37. Shepherd AJ, Mohapatra DP. Tissue preparation and immunostaining of mouse sensory nerve fibers innervating skin and limb bones. *J Visualiz Experim*. 2012;e3485. doi:10.3791/3485

38. Burnett SH, Kershen EJ, Zhang J, et al. Conditional macrophage ablation in transgenic mice expressing a Fas-based suicide gene. *J Leukoc Biol*. 2004;75:612–623. doi:10.1189/jlb.0903442

39. Clifford AB, Elnaggar AM, Robison RA, O'Neill K. Investigating the role of macrophages in tumor formation using a MaFIA mouse model. *Oncol Rep*. 2013;30:890–896. doi:10.3892/or.2013.2508

40. Shutov LP, Warwick CA, Shi X, et al. The complement system component c5a produces thermal hyperalgesia via macrophage-to-nociceptor signaling that requires NGF and TRPV1. *J Neurosci*. 2016;36:5055–5070. doi:10.1523/JNEUROSCI.3249-15.2016

41. Vichare R, Crelli C, Liu L, et al. Folate-conjugated near-infrared fluorescent perfluorocarbon nanoemulsions as theranostics for activated macrophage COX-2 inhibition. *Sci Rep*. 2023;13:15229. doi:10.1038/s41598-023-41959-9

42. Balogh M, Zhang J, Gaffney CM, et al. Sensory neuron dysfunction in orthotopic mouse models of colon cancer. *J Neuroinflammation*. 2022;19:204. doi:10.1186/s12974-022-02566-z

43. Müller DA, Snedeker JG, Meyer DC. Two-month longitudinal study of mechanical properties of absorbable sutures used in orthopedic surgery. *J Orthopaedic Surg Res*. 2016;11:111. doi:10.1186/s13018-016-0451-5

44. Baptista AF, Gomes JRDS, Oliveira JT, et al. A new approach to assess function after sciatic nerve lesion in the mouse—Adaptation of the sciatic static index. *J Neurosci Meth*. 2007;161:259–264. doi:10.1016/j.jneumeth.2006.11.016

45. Vasudeva K, Andersen K, Zeyzus-Johns B, et al. Imaging neuroinflammation in vivo in a neuropathic pain rat model with near-infrared fluorescence and (1)(9)F magnetic resonance. *PLoS One*. 2014;9:e90589. doi:10.1371/journal.pone.0090589

46. Espagnolle N, Balguerie A, Arnaud E, Sensebé L, Varin A. CD54-mediated interaction with pro-inflammatory macrophages increases the immunosuppressive function of human mesenchymal stromal cells. *Stem Cell Reports*. 2017;8:961–976. doi:10.1016/j.stemcr.2017.02.008

47. Jang E, Lee S, Kim J-H, et al. Secreted protein lipocalin-2 promotes microglial M1 polarization. *FASEB j*. 2013;27:1176–1190. doi:10.1096/fj.12-222257

48. Satoh J-I. Gene expression profiles of M1 and M2 microglia characterized by comparative analysis of public datasets. *Clin Experim Neuroimmunol*. 2018;9:124–138. doi:10.1111/cen3.12426

49. Hoffmann A, Kralisch S, Duhring S, et al. Effects of leptin on macrophages in vivo. *Atherosclerosis*. 2014;235:e194. doi:10.1016/j.atherosclerosis.2014.05.572

50. Lew HL, Otis JD, Tun C, et al. Prevalence of chronic pain, posttraumatic stress disorder, and persistent postconcussive symptoms in OIF/OEF veterans: polytrauma clinical triad. *J Rehabil Res Dev*. 2009;46:697–702. doi:10.1682/JRRD.2009.01.0006

51. Garrity R, Arora N, Haque MA, et al. Fibroblast-derived PI16 sustains inflammatory pain via regulation of CD206(+) myeloid cells. *Brain Behav Immun*. 2023;112:220–234. doi:10.1016/j.bbi.2023.06.011

52. Gabay E, Tal M. Pain behavior and nerve electrophysiology in the CCI model of neuropathic pain. *Pain*. 2004;110:354–360. doi:10.1016/j.pain.2004.04.021

53. Kennedy DL, Kemp HI, Ridout D, Yarnitsky D, Rice ASC. Reliability of conditioned pain modulation: a systematic review. *Pain*. 2016;157:2410–2419. doi:10.1097/j.pain.0000000000000689

54. Kucharczyk MW, Derrien D, Dickenson AH, Bannister K. The stage-specific plasticity of descending modulatory controls in a rodent model of cancer-induced bone pain. *Cancers*. 2020;12:3286. doi:10.3390/cancers12113286

55. Pitzer C, Kurpiers B, Eltokhi A. Gait performance of adolescent mice assessed by the CatWalk XT depends on age, strain and sex and correlates with speed and body weight. *Sci Rep*. 2021;11:21372. doi:10.1038/s41598-021-00625-8

56. Chen YJ, Cheng F-C, Sheu M-L, et al. Detection of subtle neurological alterations by the Catwalk XT gait analysis system. *J Neuroeng Rehabil*. 2014;11:62. doi:10.1186/1743-0003-11-62

57. Vrinten DH, Hamers FF. 'CatWalk' automated quantitative gait analysis as a novel method to assess mechanical allodynia in the rat; a comparison with von Frey testing. *Pain*. 2003;102:203–209. doi:10.1016/s0304-3959(02)00382-2

58. Ristoiu V. Contribution of macrophages to peripheral neuropathic pain pathogenesis. *Life Sci*. 2013;93:870–881. doi:10.1016/j.lfs.2013.10.005

59. Shepherd AJ, Copits BA, Mickle AD, et al. Angiotensin II triggers peripheral macrophage-to-sensory neuron redox crosstalk to elicit pain. *J Neurosci*. 2018;38:7032–7057. doi:10.1523/JNEUROSCI.3542-17.2018

60. Xie W, Strong JA, Meij JTA, Zhang JM, Yu L. Neuropathic pain: early spontaneous afferent activity is the trigger. *Pain*. 2005;116:243–256. doi:10.1016/j.pain.2005.04.017

61. Janjic JM, Gorantla VS. Peripheral Nerve Nanoimaging: monitoring Treatment and Regeneration. *AAPS J*. 2017;19:1304–1316. doi:10.1208/s12248-017-0129-x

62. Rosen S, Ham B, Mogil JS. Sex differences in neuroimmunity and pain. *J Neurosci Res*. 2017;95:500–508. doi:10.1002/jnr.23831